From deep brain phenotyping to functional atlasing

Bertrand Thirion, Alexis Thual, Ana Luísa Pinho

From deep brain phenotyping to functional atlasing

Bertrand Thirion[1], Alexis Thual[1,2], and Ana Luísa Pinho[1]

[1]*Université Paris-Saclay, Inria, CEA, Palaiseau, 91120, France*
[2]*Inserm, Collège de France, Paris, France*

Abstract

How can neuroimaging inform us about the function of brain structures? This simple question immediately brings out two pertinent issues: *(i)* an inference problem, namely the fact that the function of a region can only be asserted after observing a large array of experimental conditions or contrasts; and *(ii)* the fact that the identity of a region can only be defined with accuracy at the individual level, because of intrinsic differences between subjects. To overcome this double challenge, we consider an approach based on the deep phenotyping of behavioral responses from task data acquired using functional Magnetic Resonance Imaging. The concept of *functional fingerprint*—which subsumes the accumulation of functional information at a given brain location—is herein discussed in detail through concrete examples taken from the *Individual Brain Charting* dataset.

Highlights

- The accumulation of functional contrasts results in a univocal characterization of brain regions, called *functional fingerprint*.
- Distributed functional responses can be captured in dictionaries of functional fingerprints.
- Dictionaries of fingerprints constitute a three-way brain model: functional specialization, connectivity and topography of brain structures.
- Dictionaries of fingerprints can be defined at the individual level, leading to subject-specific topographies.

1 Introduction

So far, *functional Magnetic Resonance Imaging* (fMRI), has mostly been used in cognitive neuroscience to observe differential responses to cognitive tasks across brain regions. These differential responses, called *functional contrasts*, are usually reported at the population level in the literature. Representative brain maps are either described in terms of peaks of activation or shared as data derivatives in public repositories, like *NeuroVault* [GVR+15]. The accumulation of such maps brings very useful information on the neural correlates underlying cognitive operations, yet they do not allow for conclusions about the specific function of brain regions [Hen06, VSP+18].

In the last decade, a further line of research relying on resting-state fMRI data has emerged with the main purpose of providing fine delineations of macro-scale structures (regions or networks) and hence deliver new insights on brain organization; it is framed as *connectome analysis*. Indeed, studies involving connectome analysis in humans have been fostered by large-scale initiatives, like the *Human Connectome Project* (HCP). Some of these efforts have focused on the demarcation of brain structures using information from resting-state fMRI as wall as other neuroimaging modalities [GCR+16]. Such topographical mapping outlines brain regions [CFD+08] or networks [SFM+09, YKS+11, BVG+16] that can be grouped in brain atlases [GCR+16, SKG+17]. Another view on brain topography conceptualizes instead cortical organization in terms of large-scale gradients [MGG+16].

One of the current challenges is thus to bridge the information brought by both functional connectivity analysis and functional contrasts [BVG+16]. Such integration is done much more accurately at the intra-subject level [PAF+21], considering that large inter-individual variations related to location, magnitude or spatial organization of functional contrasts or functional connectivity can only yield blurred models at the population level.

To summarize, a functional atlas of the human brain should be informative with respect to three main features: *(i)* the topographical structure of the selected regions or networks; *(ii)* the functional identity of the extracted structures; and *(iii)* the connectivity underlying the signals observed among these structures.

In this paper, we outline an approach based on the accumulation of contrast maps in few individuals, wherein we discuss and illustrate the concept of functional fingerprint. This is based on the *Individual Brain Charting* (IBC) dataset [PAR+18, PAG+20], a high-resolution task-fMRI dataset acquired in a fixed environment and fixed cohort of twelve subjects. The IBC dataset provides a comprehensive collection of contrasts that aims at characterizing the cognitive components underlying a very large collection of tasks, along with high-resolution anatomical information. FMRI data are acquired at 1.5mm isotropic resolution (see [PAR+18] for more details). This dataset currently features approximately 150 task-fMRI contrasts, together with passive watching of visual and auditory naturalistic scenes, as well as anatomical contrasts. It thus constitutes an unprecedented opportunity to test the feasibility of performing both individual- and population-based functional atlasing through the description of regional fingerprints.

2 From Contrast Maps to Functional Fingerprints

The accumulation of functional contrasts at the individual level allows for a subject-specific description of the functional properties of brain territories. More precisely, the functional specificity of brain regions can be captured through the conjunction of many contrasts; for instance, the visual word form area can be functionally characterized as an area which responds to visual objects in general, but more to language content than other visual categories [DC11].

The benefits resulting from the accumulation of contrast maps have been explored in few studies. Some recent large-scale mapping efforts, such as the *Archi* [PTM+07, PdD+19] and HCP datasets [BBH+13, GCR+16], aimed at a complete characterization of a few cognitive networks, according to their implication in task performance as well as their variability at the population level. However the cognitive coverage of such datasets is typically restricted to a handful of tasks, ultimately limiting the number of available contrasts to a few dozens at best. Acquiring *naturalistic stimuli* can help to broaden the scope of such studies. As an example, the *StudyForrest* initiative has produced a set of openly available multi-modal datasets featuring fMRI data on the continuous presentation of scenes included in the "Forrest Gump" movie. This project has thus launched sev-

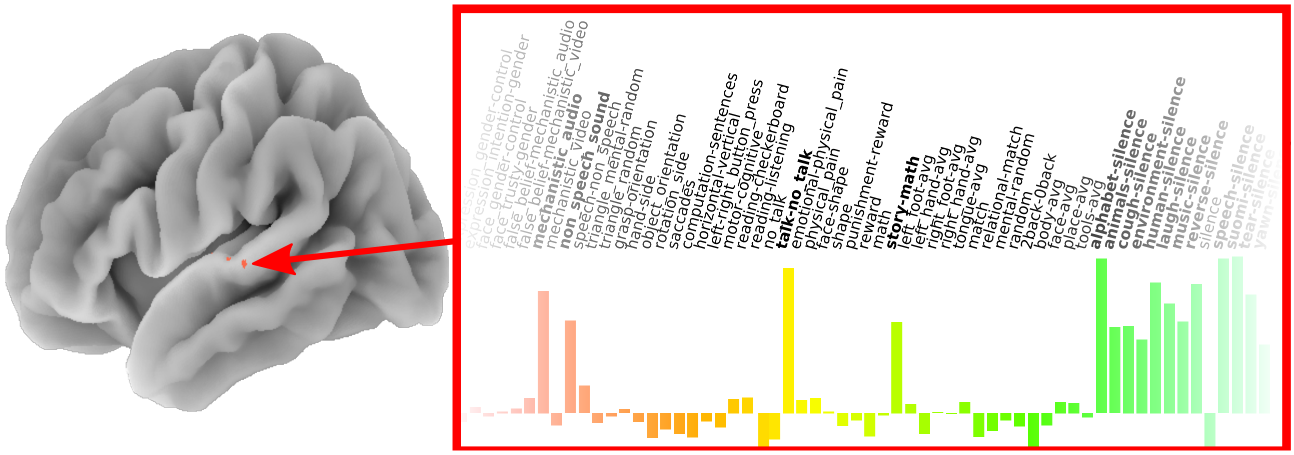

Figure 1: **What is a functional fingerprint?** A functional prototype or functional fingerprint is a vector of response to a set of contrasts in a given brain location or brain region. It characterizes the profile of functional response to a possibly wide array of experimental conditions in that particular region. In this example, we observe that the voxel considered obtains large responses to conditions involving sounds and, specifically, voice content.

eral studies investigating the neurocognitive encoding of complex auditory and visual information, by modeling specific audio and visual properties of the stimuli [HBI+14, HDH+15, HAK+16, SKG+16]. Nonetheless, such approaches forgo the simplicity and the interpretability of contrast-based mapping.

On the other hand, recent neuroimaging studies have started to adopt *individual analysis* in order to mitigate the negative impact of both functional and anatomical inter-subject variability on the precise demarcation of brain territories [FBK11, HGC+11, NCF12, FG12, HBI+14, LGA+15, HdHG+16, HLN+16, BB17, GLG+17, CPM+19]. However, they typically refer to single task studies, that only probe very specific cognitive mechanisms. Among those, the IBC dataset consists in an extensive collection of task data, targeting an exhaustive and spatially accurate characterization of individual cognitive networks. To this end, the dataset yields an extensive collection of contrasts that span a large number of cognitive components. Its successive releases [PAR+18, PAG+20] pertain foremost to:

(i) data acquired from localizers (task batteries), whose conditions range from perception to higher-order thinking skills [PTM+07, BBH+13];

(ii) data from a rapid-serial-visual-presentation paradigm on language comprehension [HBML06, PAR+18];

(iii) data on specific cognitive tasks, such as mental time and space navigation [GPvW18], reward [LADP15], theory-of-mind [DFKHBS11], pain [JBKHS16], numerosity [KPS+14], self-reference effect [GBC+14], and speech recognition [CSW+15];

(iv) an auditory task, tackling different kinds of naturalistic auditory stimuli;

(v) and retinotopic mapping.

Here, we consider a collection of 149 independent contrasts that were obtained from the task data of the first three releases (see section A). With these data, we then propose to operationalize the concept of functional fingerprinting [GRL+18] illustrated in Figure 1: fingerprints refer to a vector of activation values that define the functional prototype of a certain region of interest.

3 Discovering structure among functional prototypes

Deriving a principled description of such functional signatures across brain regions is not trivial. Indeed, as noted e.g. in [LVKG10], some arbitrariness arising from modeling choices might obfuscate the intrinsic organization of the brain. Data-driven methods can thus be better suited to capturing the essence of such inner representations. They mostly rely on *clustering* [LVKG10, YKS+11, YKE+16] or decomposition methods, such as *Independent Components Analysis* (ICA) [SFM+09] or *Dictionary Learning* [VSPT13, BVG+16]. These approaches broadly consist in factorizing the set of functional signatures collected across locations and, potentially, across individuals. Note that all these methods entail some kind of ill-posed model selection, in order to tune the hyper-parameters. Although this issue is not discussed in detail herein, we mostly recommend avoiding overly complex models, that might induce overfit, and using methods' default parameters whenever possible.

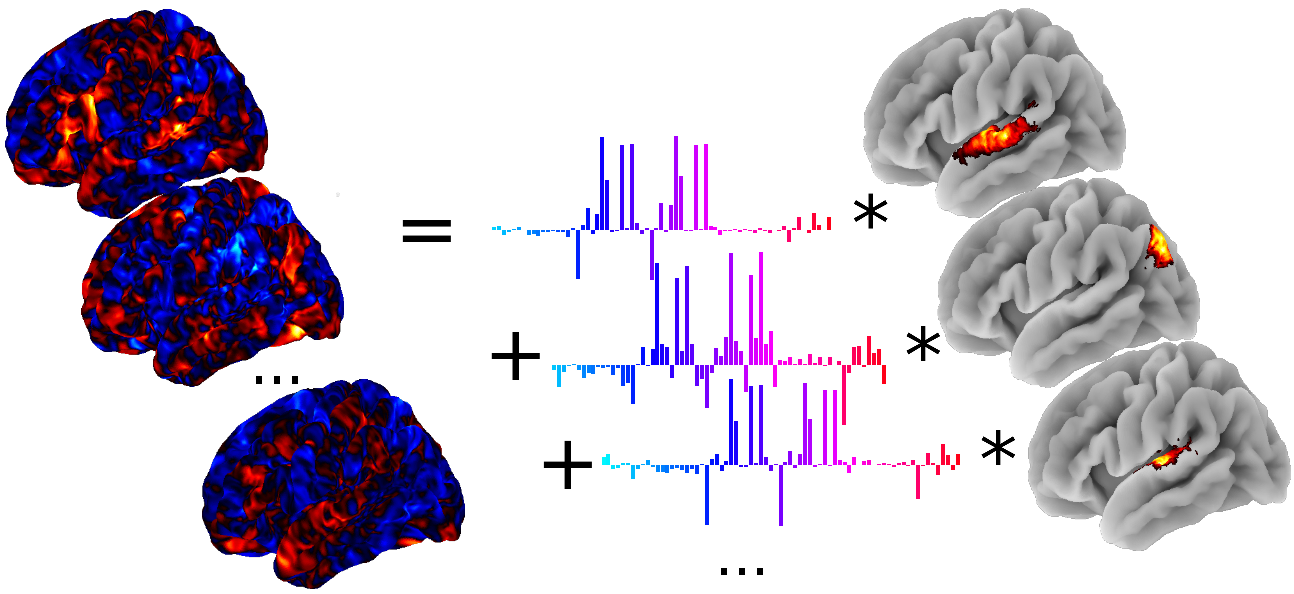

Figure 2: **Principle of Dictionary Learning** A set of 149 contrast images corresponding to distinct contrasts *(left)* can be factorized into a set of functional profiles multiplied by sparse non-negative topographies *(right)*. This latent-factor data model yields an efficient description of the brain maps used as inputs. The sparsity of the obtained topographies allows for a better characterization of the ensuing networks, while functional profiles yield a precise specification of their functional role. This factorization can be easily extended to multi-subjects settings [VSPT13].

In this article, we focus on Dictionary Learning, which stands as an intermediate between ICA and Clustering. Similar to ICA, Dictionary Learning follows a linear decomposition approach that fits well the signal. Similar to clustering, Dictionary Learning provides clear delineations of brain structures. In recent work

[BVG+16, DMVT16], it has been shown to yield good representations for fMRI data.

We follow the functional approach to multi-subject Dictionary Learning, as described in [VSPT13] and [PAF+21]. This outputs the factorization of individual contrast maps into a dictionary of cognitive profiles common to all subjects, plus subject-specific spatial maps. Sparsity is enforced with a penalty on the loadings of the components, together with a non-negativity constraint (see Figure 2). A formal description of the procedure is drawn in section C. Given a set of input images, it returns a set of non-negative and sparse topographies associated with functional fingerprints; these jointly summarize the input data.

As shown in [PAF+21] by a bootstrap analysis, a clear benefit of distilling functional maps into such a dictionary is that the topography of the resulting components is more stable than that of the underlying contrast maps. This makes dictionary decompositions more robust to inter-subject variability.

4 Topography, connectivity and functional specialization

We illustrate the result of applying Dictionary Learning to the IBC contrast maps in Figure 3. Based on a set of $c = 149$ contrast maps available in $n = 11$ subjects, we derived $k = 20$ networks using a dictionary-learning technique as described in [PAF+21]. Each network is characterized by its connectivity to other networks as well as by its functional signature. Here, the functional signature is coarsely summarized by the names of the two contrasts eliciting the highest activation in the underlying network. Note that this may sometimes outline arbitrarily some contrasts that have a higher signal-to-noise ratio. Improving such descriptions is therefore a relevant topic for future research.

Moreover, the connectivity among these networks can be computed as the partial correlation between the average activity within these networks.

Overall, derived networks show good coverage not only for the sensory and motor areas—the visual system is notably divided into its ventral and dorsal pathways and different motor regions are clearly distinguished—but also the default-mode, saliency and executive-control networks. The coverage of the prefrontal lobe is lower, indicating less consistency across subjects in the corresponding regions. Most components display cross-hemisphere symmetry, except for the left-lateralized language component and the right-lateralized attentional fronto-parietal network.

The connectome among these 20 components was obtained by computing the partial correlations among the functional fingerprints. In spite of the sparse prior used for estimating partial correlations, the network is densely connected, showing a very ordered structure across networks. For instance, the bilateral network associated with tongue motion (in red) has a strong partial connectivity with networks that are involved in speech ("reversed speech" and "letters sounds", in green), listening to or reading stories ("tale" and "read words", in yellow), and response to mental time travel's events presented in auditory modality ("response to events", in pink), although those are not necessarily close in brain space.

5 Inter-individual variability in the obtained topographies

Connectome-type analyses enable whole-brain as well as regional brain comparisons. The individual topographies derived from these methods highlight the fact that shape, size and position of functional signatures in brain territories differ from one subject to another [GLG+17, GLN+18, KLO+19, GMG+20], although the large-scale organization of the human brain is considered to be consistent across individuals. These topographic differences are important, as they lay the groundwork to study inter-individual characteristics [SNV+15, MAAB+16, BWG+18]. Capturing individual properties through the connectome can even lead to the unique identification of individuals [FSS+15].

Nevertheless, functional mapping enables a more straightforward access to inter-individual variability, namely the one that can be identified in contrast maps. The major challenge when capturing such variability lies in teasing apart actual topographic variability from noise [VSPT13]. To address this problem, *functional-correspondence Dictionary Learning* is used as it consists in the application of Dictionary Learning to data concatenated along the voxel dimension, thus enforcing functional correspondence across individuals [VSPT13]. Such a model does not impose any spatial correspondence which is ideal to uncover patterns of spatial similarities/dissimilarities between subjects.

Figure 4 illustrates the brain networks obtained from the IBC dataset using the same setting as in the previous section. Although the global topographic organization is well-preserved across individuals, inter-individual variability stands out as a major feature. Imputing this variability to actual inter-individual differences or to noise constitutes a non-trivial issue and it cannot be well-addressed in a small sample. Therefore, the relevance of these maps can be assessed through the fit of other neuroimaging variables, like cortical thickness or myelin distribution, as well as non-neuroimaging ones, like behavioral scores.

The results reported in Figure 4 show a relatively ordered structure in the occipital, temporal and parietal lobes, in contrast with the large variability present in frontal regions; such variability is particularly evident in the right frontal lobe, which appears to be almost unstructured. In the left hemisphere, the consistency of the language network creates a more stable representation.

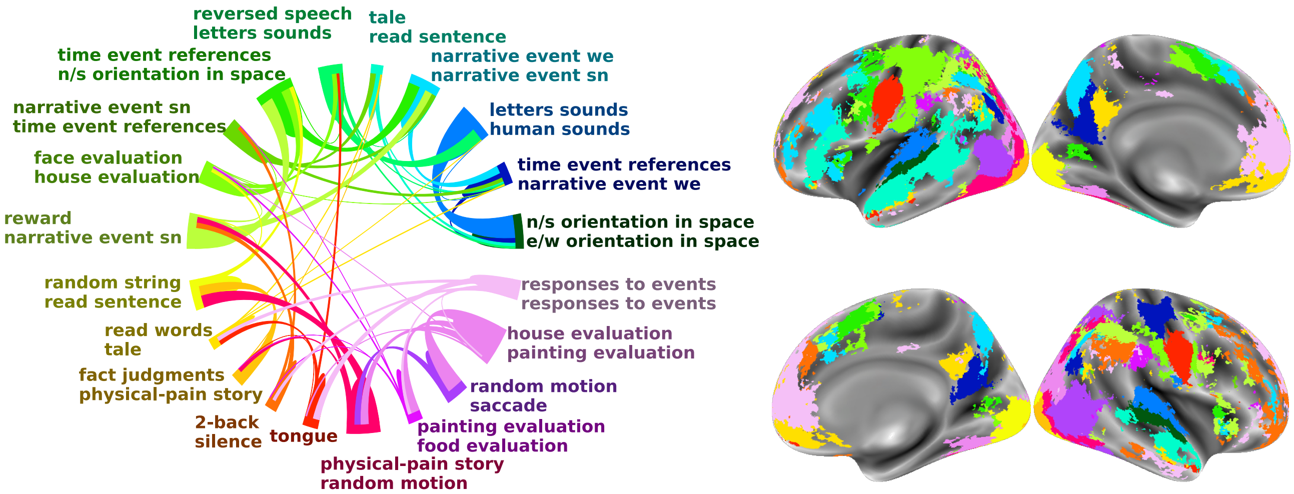

Figure 3: **Identifying suitable network descriptions of the brain.** From 149 contrast maps available in 11 subjects, we derive $k = 20$ networks in a data-driven way. *(left)* Each network is characterized by its functional connectivity to other networks as well as by a functional signature. The functional signature is summarized by the names of the two contrasts that elicit most activation in that particular network. Using activation or resting-state data, the connectivity among these networks is captured by partial correlations among the regional signals. *(right)* The networks are also characterized by topographic maps, summarized herein by their cortical representation.

As this asymmetry is, to the best of our knowledge, not fully accounted for by previous resting-state-based network studies, it suggests further comparisons between the network structure implied by such contrasts versus those observed with resting-state studies. We defer that question to future work. Moreover, as surface-based alignment is thought to provide state-of-the-art alignment of individual anatomical organization, a great deal of functional variability remains, which clearly points to variable underlying function of brain regions across individuals. Once again, this deserves more investigation.

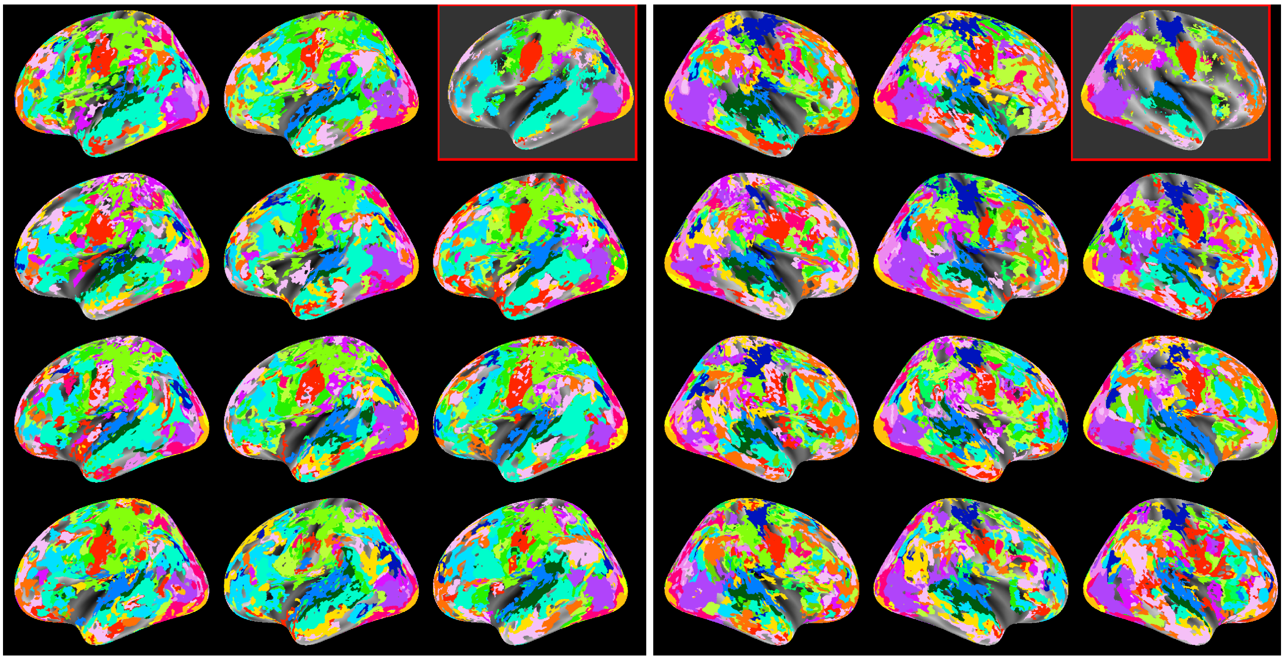

Figure 4: **Variability of individual topographies pertaining to task-elicited brain responses.** Based on the decomposition of a set of contrast maps in 11 subjects, we define 20 networks through a data-driven procedure. The resulting topographies are mapped on the left and right hemispheres of the cortex. The cross-subject consensus maps are shown at the top-right corner of both panels; they are identical to those displayed on Figure 3. Individual topographies show conspicuous variability across individuals, although the large-scale organization remains consistent.

6 Discussion

The dictionary-learning strategy outlined herein provides a qualitative assessment of the spatial organization of brain function: first, by providing synthetic summaries of the system-level organization of the brain; second, by outlining the differences across individuals. Bearing these intuitions in mind and proceeding toward a systematic analysis, the next step is to assess quantitatively the information conveyed by this functional fingerprint representation. This could be done by assessing *external validity* of the employed features, which involves typically involves some kind of generalization (see e.g. [VP19]): *predicting* some feature of brain organization that can be checked with unseen data gives an arguably stronger evidence for these observations. For instance, can one predict the precise location of the visual word form area in a given individual based on such functional fingerprints? If yes, this would lay the ground for automatic regions identification from fingerprints. Such approach was pursued by [GCR+16], though the ground truth was based on non-replicable expert-supplied segmentation.

Another implication of the functional fingerprint concept is the possibility to impute non-observed contrasts, given some observed ones. This framework has been used to predict task contrasts from either resting-state topographies [TJM+16] or other task-fMRI contrasts [TVG+14, PAF+21]. The interest of this type of prediction is to open the possibility to generalize the information from cohorts comprising a few densely sampled subjects to cohorts that share some common contrasts, e.g. from the IBC to the whole HCP cohort.

Here, we have considered only task-fMRI contrasts, but including more functional features from naturalistic stimuli and resting state as well as anatomical features would bring complementary information worth of further investigation. Finding the correct generalization of the fingerprint concept to different types of information, such as *connectional fingerprints*, is still an open question. We note that, while it is a common hypothesis that connectivity underlies function (among others, see [SOK+12]), the link between connectivity and functional fingerprints [GRL+18] is still elusive.

Finally, we have noticed in section 4 that it was helpful to annotate each functional fingerprint with proper cognitive terms; yet we have only relied on the contrasts referring to the largest functional responses for the considered component. A finer functional characterization asks for defining proper ontologies in cognitive neuroscience [PKK+11, PY16]. Such formal representations can then provide annotations that better define the function of brain areas.

Acknowledgements. This project/research has received funding from the European Union's Horizon 2020 Framework Program for Research and Innovation under the Specific Grant Agreement No. 945539 (Human Brain Project SGA3).

References

[APE+14] Alexandre Abraham, Fabian Pedregosa, Michael Eickenberg, Philippe Gervais, Andreas Mueller, Jean Kossaifi, Alexandre Gramfort, Bertrand Thirion, and Gaë Varoquaux. Machine learning for neuroimaging with scikit-learn. *Front Neuroinform*, 8:14, 2014.

[ASA03] Jesper L.R. Andersson, Stefan Skare, and John Ashburner. How to correct susceptibility distortions in spin-echo echo-planar images: application to diffusion tensor imaging. *Neuroimage*, 20(2):870 – 888, 2003.

[BB17] Rodrigo M. Braga and Randy L. Buckner. Parallel Interdigitated Distributed Networks within the Individual Estimated by Intrinsic Functional Connectivity. *Neuron*, 95(2):457–471.e5, July 2017.

[BBH+13] Deanna M Barch, Gregory C Burgess, Michael P Harms, Steven E Petersen, Bradley L Schlaggar, Maurizio Corbetta, Matthew F Glasser, Sandra Curtiss, Sachin Dixit, Cindy Feldt, Dan Nolan, Edward Bryant, Tucker Hartley, Owen Footer, James M Bjork, Russ Poldrack, Steve

Smith, Heidi Johansen-Berg, Abraham Z Snyder, and David C Van Essen. Function in the human connectome: Task-fMRI and individual differences in behavior. *Neuroimage*, 80:169–89, October 2013.

[BRLL07] Yashar Behzadi, Khaled Restom, Joy Liau, and Thomas T. Liu. A component based noise correction method (compcor) for {BOLD} and perfusion based fMRI. *Neuroimage*, 37(1):90 – 101, 2007.

[BVG+16] Danilo Bzdok, Gaël Varoquaux, Olivier Grisel, Michael Eickenberg, Cyril Poupon, and Bertrand Thirion. Formal Models of the Network Co-occurrence Underlying Mental Operations. *PLoS Comput Biol*, June 2016.

[BWG+18] Janine Diane Bijsterbosch, Mark W Woolrich, Matthew F Glasser, Emma C Robinson, Christian F Beckmann, David C Van Essen, Samuel J Harrison, and Stephen M Smith. The relationship between spatial configuration and functional connectivity of brain regions. *ELife*, 7:e32992, feb 2018.

** This work shows the importance of topographic information obtained from functional neuroimaging data: its shows that much of the variability observed in functional connectivity estimates across individuals could be explained by topographic details of the underlying brain maps. In turn, such topographic differences are predictive of inter-subject characteristics. This highlights the importance of analysis methods that explicitly account for inter-subject topographic variability.

[CFD+08] A. L. Cohen, D. A. Fair, N. U. Dosenbach, F. M. Miezin, D. Dierker, D. C. Van Essen, B. L. Schlaggar, and S. E. Petersen. Defining functional areas in individual human brains using resting functional connectivity MRI. *Neuroimage*, 41(1):45–57, May 2008.

[CPM+19] Nadine Chang, John Pyles, Austin Marcus, Abhinav Gupta, Michael Tarr, and Elissa Aminoff. BOLD5000, a public fMRI dataset while viewing 5000 visual images. *Sci Data*, 6:49, 5 2019.

[CSW+15] Karen L. Campbell, Meredith A. Shafto, Paul Wright, Kamen A. Tsvetanov, Linda Geerligs, Rhodri Cusack, Lorraine K. Tyler, Carol Brayne, Ed Bullmore, Andrew Calder, Rhodri Cusack, Tim Dalgleish, John Duncan, Rik Henson, Fiona Matthews, William Marslen-Wilson, James Rowe, Meredith Shafto, Karen Campbell, Teresa Cheung, Simon Davis, Linda Geerligs, Rogier Kievit, Anna McCarrey, Darren Price, Jason Taylor, Kamen Tsvetanov, Nitin Williams, Lauren Bates, Tina Emery, Sharon Erzinçlioglu, Andrew Gadie, Sofia Gerbase, Stanimira Georgieva, Claire Hanley, Beth Parkin, David Troy, Jodie Allen, Gillian Amery, Liana Amunts, Anne Barcroft, Amanda Castle, Cheryl Dias, Jonathan Dowrick, Melissa Fair, Hayley Fisher, Anna Goulding, Adarsh Grewal, Geoff Hale, Andrew Hilton, Frances Johnson, Patricia Johnston, Thea Kavanagh-Williamson, Magdalena Kwasniewska, Alison McMinn, Kim Norman, Jessica Penrose, Fiona Roby, Diane Rowland, John Sargeant, Maggie Squire, Beth Stevens, Aldabra Stoddart, Cheryl Stone, Tracy Thompson, Ozlem Yazlik, Marie Dixon, Dan Barnes, Jaya Hillman, Joanne Mitchell, Laura Villis, and Lorraine K. Tyler. Idiosyncratic responding during movie-watching predicted by age differences in attentional control. *Neurobiol Aging*, 36(11):3045 – 3055, 2015.

[DC11] Stanislas Dehaene and Laurent Cohen. The unique role of the visual word form area in reading. *Trends Cogn Sci*, 15(6):254 – 262, 2011.

[DFKHBS11] David Dodell-Feder, Jorie Koster-Hale, Marina Bedny, and Rebecca Saxe. fMRI item analysis in a theory of mind task. *Neuroimage*, 55(2):705 – 712, 2011.

[DMVT16] Elvis Dohmatob, Arthur Mensch, Gaël Varoquaux, and Bertrand Thirion. Learning brain regions via large-scale online structured sparse dictionary-learning. In *Neural Information Processing Systems (NIPS)*, Barcelona, Spain, December 2016.

[FBK11] Evelina Fedorenko, Michael K. Behr, and Nancy Kanwishera. Functional specificity for high-level linguistic processing in the human brain. *Proc Natl Acad Sci U S A*, 108(39):16428–33, December 2011.

[FFFT95] K.J. Friston, C.D. Frith, R.S.J. Frackowiak, and R. Turner. Characterizing Dynamic Brain Responses with fMRI: a Multivariate Approach. *Neuroimage*, 2(2):166–172, 1995.

[FG12] Martin A. Frost and Rainer Goebel. Measuring structural–functional correspondence: Spatial variability of specialised brain regions after macro-anatomical alignment. *Neuroimage*, 59(2):1369 – 1381, 2012.

[FSS+15] Emily S Finn, Xilin Shen, Dustin Scheinost, Monica D Rosenberg, Jessica Huang, Marvin M Chun, Xenophon Papademetris, and R Todd Constable. Functional connectome fingerprinting: identifying individuals using patterns of brain connectivity. *Nat Neurosci*, 18(11):1664, 2015.

[FSTD99] Bruce Fischl, Martin I. Sereno, Roger B.H. Tootell, and Anders M. Dale. High-resolution intersubject averaging and a coordinate system for the cortical surface. *Hum Brain Mapp*, 8(4):272–284, 1999.

[GBC+14] Sarah Genon, Mohamed Ali Bahri, Fabienne Collette, Lucie Angel, Arnaud d'Argembeau, David Clarys, Sandrine Kalenzaga, Eric Salmon, and Christine Bastin. Cognitive and neuroimaging evidence of impaired interaction between self and memory in Alzheimer's disease. *Cortex*, 51:11 – 24, 2014.

[GCR+16] Matthew F. Glasser, Timothy S. Coalson, Emma C. Robinson, Carl D. Hacker, John Harwell, Essa Yacoub, Kamil Ugurbil, Jesper Andersson, Christian F. Beckmann, Mark Jenkinson, Stephen M. Smith, and David C. van Essen. A multi-modal parcellation of human cerebral cortex. *Nature*, 536(7615):171–178, July 2016.

[GLG+17] Evan M. Gordon, Timothy O. Laumann, Adrian W. Gilmore, Dillan J. Newbold, Deanna J. Greene, Jeffrey J. Berg, Mario Ortega, Catherine Hoyt-Drazen, Caterina Gratton, Haoxin Sun, Jacqueline M. Hampton, Rebecca S. Coalson, Annie L. Nguyen, Kathleen B. McDermott, Joshua S. Shimony, Abraham Z. Snyder, Bradley L. Schlaggar, Steven E. Petersen, Steven M. Nelson, and Nico U.F. Dosenbach. Precision Functional Mapping of Individual Human Brains. *Neuron*, 95(4):791 – 807.e7, 2017.

** This paper introduces the so-called Midnight-Club dataset, that consists in repeated MRI acquisitions on 10 participants. The paper mostly describes segmentation of the cortical surfaces into territories based on information from resting-state. It highlights the magnitude of between-subjects variability in these highly-sampled subjects. It shows that the structures segmented from fMRI data are nonetheless stable.

[GLN+18] Caterina Gratton, Timothy O. Laumann, Ashley N. Nielsen, Deanna J. Greene, Evan M. Gordon, Adrian W. Gilmore, Steven M. Nelson, Rebecca S. Coalson, Abraham Z. Snyder, Bradley L. Schlaggar, Nico U.F. Dosenbach, and Steven E. Petersen. Functional Brain Networks Are Dominated by Stable Group and Individual Factors, Not Cognitive or Daily Variation. *Neuron*, 98(2):439 – 452.e5, 2018.

[GMG+20] Deanna J. Greene, Scott Marek, Evan M. Gordon, Joshua S. Siegel, Caterina Gratton, Timothy O. Laumann, Adrian W. Gilmore, Jeffrey J. Berg, Annie L. Nguyen, Donna Dierker, Andrew N. Van, Mario Ortega, Dillan J. Newbold, Jacqueline M. Hampton, Ashley N. Nielsen, Kathleen B. McDermott, Jarod L. Roland, Scott A. Norris, Steven M. Nelson, Abraham Z. Snyder, Bradley L. Schlaggar, Steven E. Petersen, and Nico U.F. Dosenbach. Integrative and Network-Specific Connectivity of the Basal Ganglia and Thalamus Defined in Individuals. *Neuron*, 105(4):742 – 758.e6, 2020.

[GPvW18] Baptiste Gauthier, Karin Pestke, and Virginie van Wassenhove. Building the Arrow of Time... Over Time: A Sequence of Brain Activity Mapping Imagined Events in Time and Space. *Cereb Cortex*, 29(10):4398–4414, 12 2018.

[GRL+18] Sarah Genon, Andrew Reid, Robert Langner, Katrin Amunts, and Simon B. Eickhoff. How to Characterize the Function of a Brain Region. *Trends Cogn Sci*, 22(4):350–364, Apr 2018.

** This paper discusses the epistemological underpinnings of functional brain mapping. While many brain regions have been defined, a comprehensive formalization of each region's function in relation to human behavior is still lacking. Current knowledge comes from various fields, which have diverse conceptions of 'functions'. Aggregating activation data from neuroimaging studies allows one to pinpoint the involvement of a region across a range of experimental conditions. Furthermore, large-sample data can disclose covariation between brain region features and ecological behavioral phenotyping. Combining these two approaches opens a new perspective to determine the behavioral associations of a brain region, and hence its function and broader role within large-scale functional networks.

[GVR+15] Krzysztof Gorgolewski, Gaë Varoquaux, Gabriel Rivera, Yannick Schwarz, Satrajit Ghosh, Camille Maumet, Vanessa Sochat, Thomas Nichols, Russell Poldrack, Jean-Baptiste Poline, Tal Yarkoni, and Daniel Margulies. NeuroVault.org: a web-based repository for collecting and sharing unthresholded statistical maps of the human brain. *Front Neuroinform*, 9:8, 2015.

[HAK+16] Michael Hanke, Nico Adelhöfer, Daniel Kottke, Vittorio Iacovella, Ayan Sengupta, Falko R. Kaule, Roland Nigbur, Alexander Q. Waite, Florian Baumgartner, and Jörg Stadler. A studyforrest extension, simultaneous fMRI and eye gaze recordings during prolonged natural stimulation. *Sci Data*, 3, October 2016.

[HBI+14] Michael Hanke, Florian J. Baumgartner, Pierre Ibe, Falko R. Kaule, Stefan Pollmann, Oliver Speck, Wolf Zinke, and Jörg Stadler. A high-resolution 7-Tesla fMRI dataset from complex natural stimulation with an audio movie. *Sci Data*, 1, May 2014.

[HBML06] Colin Humphries, Jeffrey R. Binder, David A. Medler, and Einat Liebenthal. Syntactic and Semantic Modulation of Neural Activity During Auditory Sentence Comprehension. *J Cogn Neurosci*, 18(4):665–679, April 2006.

[HDH+15] Michael Hanke, Richard Dinga, Christian Häusler, J Swaroop Guntupalli, Michael Casey, Falko R Kaule, and Jörg Stadler. High-resolution 7-Tesla fMRI data on the perception of musical genres–an extension to the studyforrest dataset. *F1000Res*, 4:174, 2015.

[HdHG+16] Alexander Huth, Wendy de Heer, Thomas Griffiths, Frédéric Theunissen, and Jack Gallant. Natural speech reveals the semantic maps that tile human cerebral cortex. *Nature*, 532(7600):453–8, April 2016.

[Hen06] Richard Henson. Forward inference using functional neuroimaging: dissociations versus associations. *Trends Cogn Sci*, 10(2):64 – 69, 2006.

[HGC+11] James V. Haxby, J. Swaroop Guntupalli, Andrew C. Connolly, Yaroslav O. Halchenko, Bryan R. Conroy, M. Ida Gobbini, Michael Hanke, and Peter J. Ramadge. A Common, High-Dimensional Model of the Representational Space in Human Ventral Temporal Cortex. *Neuron*, 72(2):404 – 416, 2011.

[HLN+16] Alexander Huth, Tyler Lee, Shinji Nishimoto, Natalia Bilenko, An Vu, and Jack Gallant. Decoding the Semantic Content of Natural Movies from Human Brain Activity. *Front Syst Neurosci*, 10:81, 2016.

[JBKHS16] Nir Jacoby, Emile Bruneau, Jorie Koster-Hale, and Rebecca Saxe. Localizing Pain Matrix and Theory of Mind networks with both verbal and non-verbal stimuli. *Neuroimage*, 126:39 – 48, 2016.

[KLO+19] R. Kong, J. Li, C. Orban, M. R. Sabuncu, H. Liu, A. Schaefer, N. Sun, X. N. Zuo, A. J. Holmes, S. B. Eickhoff, and B. T. T. Yeo. Spatial Topography of Individual-Specific Cortical Networks Predicts Human Cognition, Personality, and Emotion. *Cereb Cortex*, 29(6):2533–2551, 06 2019.

[KPS+14] André Knops, Manuela Piazza, Rakesh Sengupta, Evelyn Eger, and David Melcher. A Shared, Flexible Neural Map Architecture Reflects Capacity Limits in Both Visual Short-Term Memory and Enumeration. *J Neurosci*, 34(30):9857–9866, 2014.

[LADP15] Maël Lebreton, Raphaëlle Abitbol, Jean Daunizeau, and Mathias Pessiglione. Automatic integration of confidence in the brain valuation signal. *Nat Neurosci*, 18(8):1159–67, 2015.

[LGA+15] Timothy O. Laumann, Evan M. Gordon, Babatunde Adeyemo, Abraham Z. Snyder, Sung Jun Joo, Mei-Yen Chen, Adrian W. Gilmore, Kathleen B. McDermott, Steven M. Nelson, Nico U.F. Dosenbach, Bradley L. Schlaggar, Jeanette A. Mumford, Russell A. Poldrack, and Steven E. Petersen. Functional System and Areal Organization of a Highly Sampled Individual Human Brain. *Neuron*, 87(3):657 – 670, 2015.

[LVKG10] D. Lashkari, E. Vul, N. Kanwisher, and P. Golland. Discovering structure in the space of fMRI selectivity profiles. *Neuroimage*, 50:1085, 2010.

[MAAB+16] Karla L Miller, Fidel Alfaro-Almagro, Neal K Bangerter, David L Thomas, Essa Yacoub, Junqian Xu, Andreas J Bartsch, Saad Jbabdi, Stamatios N Sotiropoulos, Jesper LR Andersson, Ludovica Griffanti, Gwenaëlle Douaud, Thomas W Okell, Peter Weale, Iulius Dragonu, Steve Garratt, Sarah Hudson, Rory Collins, Mark Jenkinson, Paul M Matthews, and Stephen M Smith. Multimodal population brain imaging in the UK biobank prospective epidemiological study. *Nat Neurosci*, 19(11):1523–1536, November 2016.

[MGG+16] Daniel S Margulies, Satrajit S Ghosh, Alexandros Goulas, Marcel Falkiewicz, Julia M Huntenburg, Georg Langs, Gleb Bezgin, Simon B Eickhoff, F Xavier Castellanos, Michael Petrides, et al. Situating the default-mode network along a principal gradient of macroscale cortical organization. *Proc Natl Acad Sci U S A*, 113(44):12574–12579, 2016.

[NCF12] Alfonso Nieto-Castañón and Evelina Fedorenko. Subject-specific functional localizers increase sensitivity and functional resolution of multi-subject analyses. *Neuroimage*, 63(3):1646 – 1669, 2012.

[PAF+21] Ana Luísa Pinho, Alexis Amadon, Murielle Fabre, Elvis Dohmatob, Isabelle Denghien, Juan Jesús Torre, Chantal Ginisty, Séverine Becuwe-Desmidt, Séverine Roger, Laurence Laurier, Véronique Joly-Testault, Gaëlle Médiouni-Cloarec, Christine Doublé, Bernadette Martins, Philippe Pinel, Evelyn Eger, Gaël Varoquaux, Christophe Pallier, Stanislas Dehaene, Lucie Hertz-Pannier, and Bertrand Thirion. Subject-specific segregation of functional territories based on deep phenotyping. *Hum Brain Mapp*, 42(4):841–870, 2021.

* This paper introduces several key experiments on a fraction of the IBC dataset, namely the first release. In particular, it introduces the application of dictionary learning to summarize contrast maps to topographies. It studies the stability of the dictionary components across data resamplings. It also shows that some contrast maps can be successfully reconstructed from other contrasts. Finally, it illustrates how the accumulation of functional contrasts can help to distinguish between the functional specialization of several regions taken from the language network.

[PAG+20] Ana Luísa Pinho, Alexis Amadon, Baptiste Gauthier, Nicolas Clairis, André Knops, Sarah Genon, Elvis Dohmatob, Juan Jesús Torre, Chantal Ginisty, Séverine Becuwe-Desmidt, Séverine Roger, Yann Lecomte, Valérie Berland, Laurence Laurier, Véronique Joly-Testault, Gaëlle Médiouni-Cloarec, Christine Doublé, Bernadette Martins, Eric Salmon, Manuela Piazza, David Melcher, Mathias Pessiglione, Virginie Van Wassenhove, Evelyn Eger, Gaël Varoquaux, Stanislas Dehaene, Lucie Hertz-Pannier, and Bertrand Thirion. Individual Brain Charting dataset extension, second release of high-resolution fMRI data for cognitive mapping. *Sci Data*, 7(1), 2020.

[PAR+18] Ana Luísa Pinho, Alexis Amadon, Torsten Ruest, Murielle Fabre, Elvis Dohmatob, Isabelle Denghien, Chantal Ginisty, Séverine-Becuwe, Séverine Roger, Laurence Laurier, Véronique Joly-Testault, Gaëlle Médiouni-Cloarec, Christine Doublé, Bernadette Martins, Philippe Pinel, Evelyn Eger, Gaël Varoquaux, Christophe Pallier, Stanislas Dehaene, Lucie Hertz-Pannier, and Bertrand Thirion. Individual Brain Charting, a high-resolution fMRI dataset for cognitive mapping. *Sci Data*, 5:180105, 2018.

[PdD+19] Philippe Pinel, Baudouin Forgeot d'Arc, Stanislas Dehaene, Thomas Bourgeron, Bertrand Thirion, Denis Le Bihan, and Cyril Poupon. The functional database of the ARCHI project: Potential and perspectives. *Neuroimage*, 197:527 – 543, 2019.

[PKK+11] Russell Poldrack, Aniket Kittur, Donald Kalar, Eric Miller, Christian Seppa, Yolanda Gil, D. Parker, Fred Sabb, and Robert Bilder. The Cognitive Atlas: Toward a Knowledge Foundation for Cognitive Neuroscience. *Front Neuroinform*, 5:17, 2011.

[PTM+07] Philippe Pinel, Bertrand Thirion, Sébastien Meriaux, Antoinette Jobert, Julien Serres, Denis Le Bihan, Jean-Baptiste Poline, and Stanislas Dehaene. Fast reproducible identification and large-scale databasing of individual functional cognitive networks. *BMC Neurosci*, 8:91, 2007.

[PVG+11] Fabian Pedregosa, Gaël Varoquaux, Alexandre Gramfort, Vincent Michel, Bertrand Thirion, Olivier Grisel, Mathieu Blondel, Peter Prettenhofer, Ron Weiss, Vincent Dubourg, Jake Vanderplas, Alexandre Passos, David Cournapeau, Matthieu Brucher, Matthieu Perrot, and Édouard Duchesnay. Scikit-Learn: Machine Learning in Python. *J Mach Learn Res*, 12:2825–2830, November 2011.

[PY16] Russell Poldrack and Tal Yarkoni. From Brain Maps to Cognitive Ontologies: Informatics and the Search for Mental Structure. *Annu Rev Psychol*, 67:587–612, Jan 2016.

[SFM+09] Stephen M Smith, Peter T Fox, Karla L Miller, David C Glahn, P Mickle Fox, Clare E Mackay, Nicola Filippini, Kate E Watkins, Roberto Toro, Angela R Laird, and Christian F Beckmann. Correspondence of the brain's functional architecture during activation and rest. *Proc Natl Acad Sci U S A*, 106 31:13040–5, 2009.

[SKG+16] Ayan Sengupta, Falko R. Kaule, J. Swaroop Guntupalli, Michael B. Hoffmann, Christian Häusler, Jörg Stadler, and Michael Hanke. A studyforrest extension, retinotopic mapping and localization of higher visual areas. *Sci Data*, 3, October 2016.

[SKG+17] Alexander Schaefer, Ru Kong, Evan M Gordon, Timothy O Laumann, Xi-Nian Zuo, Avram J Holmes, Simon B Eickhoff, and BT Thomas Yeo. Local-global parcellation of the human cerebral cortex from intrinsic functional connectivity mri. *Cereb Cortex*, 28(9):3095–3114, 2017.

[SNV+15] Stephen Smith, Thomas Nichols, Diego Vidaurre, Anderson Winkler, Timothy Behrens, Matthew Glasser, Kamil Ugurbil, Deanna Barch, David van Essen, and Karla Miller. A positive-negative mode of population covariation links brain connectivity, demographics and behavior. *Nat Neurosci*, 18(11):1565–1567, November 2015.

[SOK+12] Zeynep M Saygin, David E Osher, Kami Koldewyn, Gretchen Reynolds, John D E Gabrieli, and Rebecca R Saxe. Anatomical connectivity patterns predict face selectivity in the fusiform gyrus. *Nat Neurosci*, 15(2):321–327, Feb 2012.

[TJM+16] I. Tavor, O. Parker Jones, R. B. Mars, S. M. Smith, T. E. Behrens, and S. Jbabdi. Task-free MRI predicts individual differences in brain activity during task performance. *Science*, 352(6282):216–220, 2016.

[TVG+14] Bertrand Thirion, Gaël Varoquaux, Olivier Grisel, Cyril Poupon, and Philippe Pinel. Principal Component Regression predicts functional responses across individuals. In *Med Image Comput Comput Assist Interv*, Boston, United States, September 2014. Springer.

[vEGD+12] David C. van Essen, Matthew F. Glasser, Donna L. Dierker, John Harwell, and Timothy Coalson. Parcellations and Hemispheric Asymmetries of Human Cerebral Cortex Analyzed on Surface-Based Atlases. *Cereb Cortex*, 22(10):2241, 2012.

[VP19] Gaël Varoquaux and Russell Poldrack. Predictive models avoid excessive reductionism in cognitive neuroimaging. *Curr Opin Neurobiol*, 55, April 2019.

> * Predictive models refer to mathematical models of brain data that explicitly minimize prediction error based on machine learning. They can be tested without the need for modeling assumption, such as Gaussian noise. As a consequence, predictive models often are more complex, departing from maximum-likelihood estimates and fitting many unknown variables concurrently.

[VSP+18] Gaël Varoquaux, Yannick Schwartz, Russell Poldrack, Baptiste Gauthier, Danilo Bzdok, Jean-Baptiste Poline, and Bertrand Thirion. Atlases of cognition with large-scale brain mapping. *PLoS Comput Biol*, 14(11), 2018.

> * This paper discusses functional atlasing based on large-scale data, such as those available in open repositories (OpenNeuro, NeuroVault). It shows that machine learning models can capture the link between cognitive concepts and brain regions, provided that they rely on the conjunction of two mappings: encoding (brain mapping) and decoding (predictive modeling). This also shows that cognitive ontologies provide an important resource to improve this atlasing endeavour. The paper coins the necessity of validating such models across studies, to avoid fitting the idiosyncrasies of each study.

[VSPT13] Gaël Varoquaux, Yannick Schwartz, Philippe Pinel, and Bertrand Thirion. Cohort-Level Brain Mapping: Learning Cognitive Atoms to Single Out Specialized Regions. In James C. Gee, Sarang Joshi, Kilian M. Pohl, William M. Wells, and Lilla Zöllei, editors, *Inf Process Med Imaging*, volume 23, pages 438–449, Berlin, Heidelberg, 2013. Springer.

[YKE+16] B. T. Yeo, F. M. Krienen, S. B. Eickhoff, S. N. Yaakub, P. T. Fox, R. L. Buckner, C. L. Asplund, and M. W. Chee. Functional Specialization and Flexibility in Human Association Cortex. *Cereb Cortex*, 26(1):465, Jan 2016.

[YKS+11] B. T. T. Yeo, F. M. Krienen, J. Sepulcre, M. R. Sabuncu, et al. The organization of the human cerebral cortex estimated by intrinsic functional connectivity. *J Neurophysio*, 106:1125, 2011.

A List of contrasts used for the IBC data functional fingerprinting

The choice of tasks and contrasts included in the analysis follow the following principles:

(i) whenever they were available, battery-structured experiments that systematically assess brain systems with a wide arrays of conditions ranging from perception to higher-order cognition have been used;

(ii) we also used tasks probing core sensory and motor systems (auditory task tackling different kinds of naturalistic auditory stimuli, retinotopic mapping, motor mapping)

(iii) we eventually reproduced domain-specific tasks have been used to map more specific aspects of cognition, such as reading, with rapid-serial-visual-presentation paradigm on language comprehension, mental time and space navigation, reward processing, theory-of-mind, pain, numerosity, self-reference effect, and speech recognition, so far; the goal was to cover as many domains as possible, in order to probe the corresponding brain systems.

Yet, the difference between domain-general tasks and domain-specific tasks should not be over-emphasized. Localizer tasks, which are domain-general tasks, typically represent a consensual way to characterize brain functions and their neural correlates. Therefore, they tend to be less specific than those addressing a particular cognitive system. These tasks also have a battery-type organization, where multiple conditions are related in a factorial structure that helps segregating territories.

Gathering and running a large number of tasks hinges on the community ability to share existing experimental protocols. This is in general hard to achieve given the current research practices stimulus-delivery software maintenance) or labor contingencies (e.g. personnel change). Data acquisition is still ongoing, with novel protocols being added to the present IBC collection (e.g. biological motion, spatial navigation, narrative listening, movie watching, among other task batteries).

Regarding the contrasts herein employed, we have focused on the independent contrasts of the studies; they refer to the main conditions *versus* baseline, also including the corresponding baselines when they deliver meaningful information. A comprehensive description of the tasks and corresponding contrasts used in this study can be found in the IBC dataset documentation, which is available on `https://project.inria.fr/IBC/data`.

Task	Contrast	Description
archi standard	left-right button press	left vs. right hand button press
archi standard	horizontal-vertical	horizontal vs. vertical checkerboard
archi standard	computation-sentences	mental subtraction vs. sentence reading
archi standard	reading-listening	reading sentence vs. listening to sentence
archi standard	reading-checkerboard	read sentence vs. checkerboard
archi standard	motor-cognitive	button presses vs. narrative/computation
archi spatial	saccades	saccade vs. fixation

Task	Contrast	Description
archi spatial	rotation side	hand palm or back vs. fixation
archi spatial	hand-side	left or right hand vs. hand palm or back
archi spatial	object orientation	image orientation reporting
archi spatial	grasp-orientation	object grasping vs. orientation reporting
archi social	triangle random	randomly drifting triangle
archi social	triangle mental-random	mental motion vs. random motion
archi social	mechanistic video	reading a mechanistic story
archi social	mechanistic audio	listening to a mechanistic tale
archi social	false belief-mechanistic video	false-belief story vs. mechanistic story
archi social	false belief-mechanistic audio	false-belief tale vs. mechanistic tale
archi social	non speech sound	listen to natural sound
archi social	speech-non speech	listen to voice sound vs. natural sound
archi emotional	face gender-control	guess the gender from face image
archi emotional	face trusty-gender	assess face trustfulness vs. gender
archi emotional	expression gender-control	guess the gender from eyes image vs. view scrambled image
archi emotional	expression intention-gender	guess intention vs. gender from eyes image
hcp emotion	shape	shape comparison
hcp emotion	face-shape	emotional face comparison vs. shape comparison
hcp gambling	reward	gambling with positive outcome
hcp gambling	punishment-reward	negative vs. positive gambling outcome
hcp motor	tongue-avg	move tongue vs. hands and feet
hcp language	math	mental additions
hcp language	story-math	listening to tale vs. mental additions
hcp relational	match	visual feature matching vs. fixation
hcp relational	relational-match	relational comparison vs. matching
hcp social	random	random motion vs. fixation
hcp social	mental-random	mental motion vs. random motion
hcp wm	2back-0back	2-back vs. 0-back
rsvp language	consonant string	read and encode consonant strings vs. fixation
rsvp language	word-consonant string	read words vs. consonant strings
rsvp language	pseudo-consonant string	read pseudowords vs. consonant strings
rsvp language	word-pseudo	read words vs. pseudowords
rsvp language	complex-simple	read sentence with complex vs. simple syntax
rsvp language	sentence-word	read sentence vs. words
rsvp language	jabberwocky-pseudo	read jabberwocky vs. pseudowords
rsvp language	sentence-jabberwocky	read sentence vs. jabberwocky
mtt we	we average reference	updating ones position in space and time in west-east island

Task	Contrast	Description
mtt we	we all space cue	spatial cue of the next event in west-east island
mtt we	we all time cue	time cue of the next event in west-east island
mtt we	we all space-time cue	spatial vs. time cues in west-east island
mtt we	we all time-space cue	time vs. spatial cues in west-east island
mtt we	we average event	figuring out the space or time of an event in west-east island
mtt we	we space event	figuring out the position of an event in west-east island
mtt we	we time event	figuring out the time of an event in west-east island
mtt we	we space-time event	event in space vs. event in time in west-east island
mtt we	we time-space event	event in time vs. event in space in west-east island
mtt we	westside-eastside event	events occuring westside vs. eastside
mtt we	eastside-westside event	events occuring eastside vs. westside
mtt we	we before-after event	events occuring before vs. after in west-east island
mtt we	we after-before event	events occuring after vs. before in west-east island
mtt we	we all event response	motor responses performed after every event condition in the west-east island
mtt sn	sn average reference	updating ones position in space and time in south-north island
mtt sn	sn all space cue	spatial cue of the next event in south-north island
mtt sn	sn all time cue	time cue of the next event in south-north island
mtt sn	sn all space-time cue	spatial vs. time cues in south-north island
mtt sn	sn all time-space cue	time vs. spatial cues in south-north island
mtt sn	sn average event	figuring out the space or time of an event in south-north island
mtt sn	sn space event	figuring out the position of an event in south-north island
mtt sn	sn time event	figuring out the time of an event in south-north island
mtt sn	sn space-time event	event in space vs. event in time in south-north island
mtt sn	sn time-space event	event in time vs. event in space in south-north island
mtt sn	southside-northside event	events occuring southside vs. northside
mtt sn	northside-southside event	events occuring northsife vs. southside
mtt sn	sn before-after event	events occuring before vs. after in south-north island
mtt sn	sn after-before event	events occuring after vs. before in south-north island
mtt sn	sn all event response	motor responses performed after all event condition in the south-north island
preference food	food constant	evaluation of food
preference food	food linear	linear effect of food preference
preference food	food quadratic	quadratic effect of food preference
preference paintings	painting constant	evaluation of paintings

Task	Contrast	Description
preference paintings	painting linear	linear effect of paintings preference
preference paintings	painting quadratic	quadratic effect of paintings preference
preference faces	face constant	evaluation of faces
preference faces	face linear	linear effect of face preference
preference faces	face quadratic	quadratic effect of face preference
preference houses	house constant	evaluation of houses
preference houses	house linear	linear effect of houses preference
preference houses	house quadratic	quadratic effect of houses preference
theory of mind	photo	manipulation of fact judgments
theory of mind	belief-photo	belief vs. factual judgments
emotional pain	physical pain	reading physical pain story
emotional pain	emotional-physical pain	emotional vs. physical pain story
pain movie	movie pain	movie with physically painful events
pain movie	movie mental-pain	mental events vs. physically painful events
self	instructions	read instruction in form of a question
bang	talk-no talk	speech vs. non-speech sections in movie watching
bang	no talk	non-speech section in movie watching
lyon lec2	attend	response to attended text
lyon lec2	unattend	response to unattended text
lyon lec2	attend-unattend	response to attended vs. unattended text
lyon audi	silence	listen to silence
lyon audi	tear-silence	listen to tears
lyon audi	suomi-silence	listen to unknown language
lyon audi	yawn-silence	listen to yawning
lyon audi	human-silence	listen to human sounds
lyon audi	music-silence	listen to music
lyon audi	reverse-silence	listen to reversed speech
lyon audi	speech-silence	listen to speech
lyon audi	alphabet-silence	listen to letters
lyon audi	cough-silence	listen to coughing
lyon audi	environment-silence	listen to environment sounds
lyon audi	laugh-silence	listen to laugh
lyon audi	animals-silence	listen to animals
lyon visu	scrambled	view a scrambled image
lyon visu	face-scrambled	view a face image
lyon visu	characters-scrambled	view a characters
lyon visu	scene-scrambled	view a scene
lyon visu	house-scrambled	view a house
lyon visu	animal-scrambled	view an animal
lyon visu	pseudoword-scrambled	view a pseudoword
lyon visu	tool-scrambled	view a tool

Task	Contrast	Description
lyon lec1	random string	read a random string
lyon lec1	word-random string	read a word vs. a random string
lyon lec1	word-pseudoword	read a word vs. a pseudoword
lyon lec1	pseudoword-random string	read a pseudoword vs. a random string
lyon mveb	2 letters different-same	maintaining two letters vs. one
lyon mveb	4 letters different-same	maintaining four letters vs. one
lyon mveb	6 letters different-same	maintaining six letters vs. one
lyon mveb	6 letters different-2 letters different	maintaining six letters vs. two
lyon mvis	2 dots-2 dots control	maintain position of two dots vs. one
lyon mvis	4 dots-4 dots control	maintain position of four dots vs. one
lyon mvis	6 dots-6 dots control	maintain position of six dots vs. one
lyon mvis	6 dots-2 dots	maintain position of six dots vs. two
lyon moto	instructions	read instructions
lyon moto	finger right-fixation	right finger tapping vs. any movement
lyon moto	finger left-fixation	left finger tapping vs. any movement
lyon moto	foot left-fixation	move left foot vs. any movement
lyon moto	foot right-fixation	move right foot vs. any movement
lyon moto	hand left-fixation	move left hand vs. any movement
lyon moto	hand right-fixation	move right hand vs. any movement
lyon moto	saccade-fixation	saccade vs. any movement
lyon moto	tongue-fixation	move tongue vs. any movement
lyon mcse	salience left-right	looking for a symbol in left vs. right visual field
lyon mcse	low-high salience	looking for a low-salient symbol
audio	music-silence	listen to music vs. silence
audio	speech-silence	listen to speech vs. silence

B Preprocessing of the IBC data

A detailed description of the preprocessing pipeline of the IBC data is provided in [PAF+21]. Raw data were preprocessed using *PyPreprocess* (`https://github.com/neurospin/pypreprocess`).

All fMRI images, i.e. GE-EPI volumes, were collected twice with reversed phase-encoding directions, resulting in pairs of images with distortions going in opposite directions. Susceptibility-induced off-resonance field was estimated from the two Spin-Echo EPI volumes in reversed phase-encoding directions. The images were corrected based on the estimated deformation model. Details about the method can be found in [ASA03].

Further, the GE-EPI volumes were aligned to each other within every participant. A rigid-body transformation was employed, in which the average volume of all images was used as reference [FFFT95]. The anatomical and motion-corrected fMRI images were given as input to *FreeSurfer* v6.0.0, in order to extract meshes of the tissue interfaces and the sampling of functional activation on these meshes, as described in [vEGD+12]. The corresponding maps were then resampled to the fsaverage7 template of FreeSurfer [FSTD99].

FMRI data were analyzed using the *General Linear Model*. Regressors of the model were designed to capture variations in BOLD response strictly following stimulus timing specifications. They were estimated through the convolution of boxcar functions, that represent per-condition stimulus occurrences, with the canonical *Hemodynamic Response Function* (HRF). To build such models, paradigm descriptors grouped in triplets (i.e. onset time, duration and trial type) according to BIDS Specification were determined from the log files' registries generated by the stimulus-delivery software. To account for small fluctuations in the latency of the HRF peak response, additional regressors were computed based on the convolution of the same task-conditions profile with the time derivative of the HRF. Nuisance regressors were also added to the design matrix in order to minimize the final residual error. To remove signal variance associated with spurious effects arising from movements, six temporal regressors were defined for the motion parameters. Further, the first five principal components of the signal, extracted from voxels showing the 5% highest variance, were also regressed to capture physiological noise [BRLL07].

In addition, a discrete-cosine basis was included for high-pass filtering (*cutoff*=$\frac{1}{128}$Hz). Model specification was implemented using *Nilearn* [APE+14], a Python library for statistical learning on neuroimaging data (`https://nilearn.github.io`).

C Technical description of the functional correspondence dictionary-learning method

Formally, consider the set of brain maps $\mathbf{X}^s = (\mathbf{X}^s_j), j \in [c]$ obtained for $c = 149$ contrasts in a subject $s \in [n]$. By enumerating the values across a mesh of vertices, each $\mathbf{X}^s_j$ is a $p-$dimensional vector, where p is the number of vertices; $\mathbf{X}^s$ is thus a matrix of size $p \times c$. Functional-correspondence Dictionary Learning solves the following minimization problem for $\lambda > 0$:

$$\min_{(\mathbf{U}^s)_{s=1\ldots n}, \mathbf{V} \in \mathcal{C}} \sum_{s=1}^{n} \left(\|\mathbf{X}^s - \mathbf{U}^s \mathbf{V}\|^2 + \lambda \|\mathbf{U}^s\|_1 \right),$$

where $\mathbf{U}^s \geq 0\,,\ \forall s \in [n]$. Here, $\mathcal{C}$ denotes the set of matrices with row norm smaller than 1. $\mathbf{U}_s$ matrices have shape $p \times k$, whereas the functional-loading matrix $\mathbf{V}$ has shape $k \times c$, k being the number of components. Herein, we used $k = 20$. In addition, $\mathbf{V}$ describes the functional characteristics of the components. The estimated subject-specific spatial components $(\mathbf{U}^s),\ s \in [n]$ can be interpreted as individual topographies; these components may overlap, although their values are zero in most regions. This is why the median value of these components is also sparse, even without applying explicit thresholds. The λ parameter was calibrated in order to yield a sparsity of around 75%. As the estimation problem is non-convex, initialization matters; here, we created an initial $\mathbf{V}$ matrix by clustering the voxels across subjects into $k = 20$ clusters and took the normalized average of the cluster signal. This is illustrated in Figure 2.

The implementation relies on the *mini-batch k-means* and the *dictionary-learning* methods of *scikit-learn* v0.21.3 [PVG+11], a Python machine-learning library (`https://scikit-learn.org/stable/`).